Received: 22 June 2022 | Revised: 10 October 2022 | Accepted: 20 October 2022

DOI: 10.1111/ppl.13807

ORIGINAL RESEARCH

Physiologia Plantarum

The vacuolar transporter LaMTP8.1 detoxifies manganese in leaves of *Lupinus albus*

Philipp Olt[1] | Santiago Alejandro-Martinez[2] | Johann Fermum[2] | Edith Ramos[2] | Edgar Peiter[2] | Uwe Ludewig[1]

[1]Institute of Crop Science, Nutritional Crop Physiology, University of Hohenheim, Stuttgart, Germany

[2]Plant Nutrition Laboratory, Institute of Agricultural and Nutritional Sciences, Martin Luther University Halle-Wittenberg, Halle, Germany

Correspondence
Uwe Ludewig, Institute of Crop Science, Nutritional Crop Physiology, University of Hohenheim, Stuttgart, Germany.
Email: u.ludewig@uni-hohenheim.de

Funding information
Deutsche Forschungsgemeinschaft, Grant/Award Numbers: Lu673/25-1, INST271/371-1 FUGG; European Regional Development Fund, Grant/Award Number: ZS/2016/06/79740

Edited by J.K. Schjoerring

Abstract

Manganese (Mn) is an essential microelement, but overaccumulation is harmful to many plant species. Most plants have similar minimal Mn requirements, but the tolerance to elevated Mn varies considerably. Mobilization of phosphate (P) by plant roots leads to increased Mn uptake, and shoot Mn levels have been reported to serve as an indicator for P mobilization efficiency in the presence of P deficiency. White lupin (*Lupinus albus* L.) mobilizes P and Mn with outstanding efficiency due to the formation of determinate cluster roots that release carboxylates. The high Mn tolerance of *L. albus* goes along with shoot Mn accumulation, but the molecular basis of this detoxification mechanism has been unknown. In this study, we identify LaMTP8.1 as the transporter mediating vacuolar sequestration of Mn in the shoot of white lupin. The function of Mn transport was demonstrated by yeast complementation analysis, in which LaMTP8.1 detoxified Mn in *pmr1*Δ mutant cells upon elevated Mn supply. In addition, LaMTP8.1 also functioned as an iron (Fe) transporter in yeast assays. The expression of *LaMTP8.1* was particularly high in old leaves under high Mn stress. However, low P availability per se did not result in transcriptional upregulation of *LaMTP8.1*. Moreover, *LaMTP8.1* expression was strongly upregulated under Fe deficiency, where it was accompanied by Mn accumulation, indicating a role in the interaction of these micronutrients in *L. albus*. In conclusion, the tonoplast-localized Mn transporter LaMTP8.1 mediates Mn detoxification in leaf vacuoles, providing a mechanistic explanation for the high Mn accumulation and Mn tolerance in this species.

1 | INTRODUCTION

The transition metal manganese (Mn) is a common element in the earth's crust. It can exist in various oxidation states (Mn^{II} to Mn^{IV}) in the soil and is found in numerous chemical compounds that vary in solubility. Thus, plant availability of Mn depends on the soil conditions. For plant growth and reproduction, Mn is essential (McHargue, 1922). It functions in the catalytic center of the water-splitting complex of photosystem II and plays an important role as a constituent or cofactor of many enzymes (Andresen et al., 2018; Barber, 2017; Ono et al., 1992).

Although this element is essential, Mn uptake is apparently relatively poorly regulated in response to the Mn status (Alejandro et al., 2020; White & Neugebauer, 2021; White & Pongrac, 2017). In *Arabidopsis thaliana*, Mn uptake at low availability is primarily conferred by the natural resistance-associated macrophage protein1 (AtNRAMP1), which is located in the root plasma membrane and takes up Mn^{2+} with high affinity, but also transports iron (Fe; Cailliatte

et al., 2010; Castaings et al., 2016). Transporters of the NRAMP family are also involved in other Mn transport processes in the plant, in particular serving intracellular distribution (He et al., 2021). Another protein involved in Mn uptake is the Fe transporter iron-regulated transporter1 (IRT1) that, besides Fe, is also permeable for cadmium, cobalt, zinc, and Mn (Korshunova et al., 1999; Rogers et al., 2000; Vert et al., 2002). The uptake of Mn is thus realized by nonspecific cation transporters that are often regulated in response to the nutritional status of elements other than Mn (White & Neugebauer, 2021). This does not only complicate the plant's response to Mn-deficient conditions but also impedes its response to excess Mn availability. Especially in soils with a low pH or under flooded conditions, high Mn availability can pose a problem to plants. The concentration of plant-available Mn in the rhizosphere soil solution can also rise to high levels as a consequence of the plant's response to deficiencies of other nutrients, such as Fe or P.

Phosphate (P) is often limiting for growth and yield formation of crops (Buczko et al., 2018). To improve P acquisition, plants employ a wide range of morphological and physiological adaptations (Peiter, 2014). In response to P deficiency, many plant species acidify the rhizosphere and release root exudates, such as carboxylates and phenolics, that mobilize P from sparingly soluble compounds (Dinkelaker et al., 1997). Simultaneously, these processes of acidification, chelation, and reduction render metals, such as Mn, more plant-available. Since Mn uptake is not strongly regulated, P deficiency-induced carboxylate exudation is strongly correlated with Mn accumulation (Lambers et al., 2015; Lambers et al., 2021). Physiological responses to Fe deficiency, such as rhizosphere acidification, also cause an increased Mn influx (Eroglu et al., 2016). All those conditions of excessive Mn availability require plants to develop strategies to avoid toxicity.

Following uptake, Mn is translocated efficiently to the shoot (Loneragan, 1988; Rengel, 2000). Toxicity symptoms typically occur at first in the lower, older leaves and spread subsequently to the upper, younger leaves (Horiguchi, 1988). Toxic concentrations of Mn cause leaf puckering, marginal chlorosis and necrosis of leaves, and Mn toxicity has been suggested to be related to various aberrances in apoplast and cytoplasm (Alejandro et al., 2020). The tolerance to high Mn and the strategies to counter this problem differ between plant species and circumstances.

In *A. thaliana*, a constitutive mechanism of Mn detoxification involves the secretion of the metal from the cytosol, whereby Mn is loaded into a Golgi compartment by metal tolerance protein11 (MTP11), a transporter of the cation diffusion facilitator (CDF) family (Peiter et al., 2007). Proteins of this family also mediate Mn detoxification by sequestration into vacuoles. In *A. thaliana*, MTP8 plays such a role specifically under Fe deficiency, which causes an increased Mn influx (Eroglu et al., 2016). Thereby, the expression of *MTP8* is massively upregulated in cortical and rhizodermal cells of the root that also express the poorly selective Fe transporter *IRT1*. This upregulation is governed by the Fe deficiency-induced transcription factor FIT, rather than by high Mn load per se. In the absence of MTP8, Fe(III) reduction by FRO2 is inhibited (Eroglu et al., 2016). Arabidopsis MTP8 is regulated by phosphorylation of serine residues at its N-terminal domain by calcium-dependent protein kinases (CPK 4/5/6/11; Zhang et al., 2021) and calcineurin B-like proteins (CBL2/3) and their interacting kinases (CIPK3/9/26; Ju et al., 2022). In Arabidopsis, MTP8 has a further role in mediating Mn storage in vacuoles of subepidermal cells of developing embryos (Eroglu et al., 2017; Höller et al., 2022). Besides Mn, MTP8 transports Fe, which appears to be relevant for the storage of remobilized Fe during imbibition and germination (Eroglu et al., 2017). Orthologs of AtMTP8 have been described in other species. The first Mn-transporting CDF protein, ShMTP1 was discovered in the tropical legume species *Stylosanthes hamata*, which is relatively Mn-tolerant (Delhaize et al., 2003). It was later renamed to ShMTP8 to conform to the nomenclature for *A. thaliana* (Montanini et al., 2007). Albeit vacuolar localization and ability to transport Mn upon heterologous expression in yeast were demonstrated, the expression pattern and physiological role of ShMTP8 remain to be studied (Delhaize et al., 2003). In rice (*Oryza sativa*), the orthologue OsMTP8.1, also localized to the tonoplast, is expressed in shoots, and its expression is related to enhanced Mn accumulation and tolerance (Chen et al., 2013), which indicates a functional difference to AtMTP8. In contrast to the localization of MTP8 orthologues in the tonoplast of *Arabidopsis* and rice (Chen et al., 2013; Eroglu et al., 2016), HvMTP8 of barley (*Hordeum vulgare*) has been allocated to the Golgi apparatus, albeit in a heterologous expression system (Pedas et al., 2014).

In a comparative study, a high Mn sensitivity of soybean (*Glycine max*) was associated with a high abundance of Mn in the plant veins but low sequestration in vacuoles or other compartments of mesophyll cells (Blamey et al., 2015). Narrow-leaved lupin (*Lupinus angustifolius*) and white lupin, on the contrary, considered as highly Mn-tolerant plant species, effectively allocated Mn to vacuoles for sequestration and conversion to metabolically inactive chelate complexes (Blamey et al., 2015). These two strategies are commonly associated with Mn tolerance in many tolerant species (Blamey et al., 2018).

Though Mn detoxification is of crucial importance for white lupin under P deficiency, the mechanism of Mn sequestration into leaf vacuoles is unknown. We hypothesized that the characteristic high Mn accumulation in white lupin may be conferred by an ortholog of MTP8 expressed in the shoot. We, therefore, identified and functionally characterized LaMTP8.1 in yeast cells, determined the subcellular localization of the protein, and analyzed the dependency of its tissue-specific expression on nutrient supply levels. Collectively, the data support a role of this protein in Mn homeostasis by vacuolar sequestration not only under high Mn load, but also, as in Arabidopsis, under Fe deficiency. However, unlike in Arabidopsis, *LaMTP8.1* was not specifically upregulated in roots but particularly in older leaves, which provides a mechanistic explanation of the extreme Mn accumulation in this tissue. Despite this likely importance to detoxify Mn mobilized by P deficiency-induced exudation of carboxylates, expression of *LaMTP8.1* was not directly regulated by the plant's P status. *LaMTP8.2*, a homolog of *LaMTP8.1*, was much lower expressed and thus may play a less important role.

TABLE 1 Nutrient solution specialized for *Lupinus albus* (Kania et al., 2003; Wang et al., 2015) modified for treatments with P, Mn, and Fe deficiency

Chemical	Control	P-deficiency	Mn-deficiency	Fe-deficiency
$Ca(NO_3)_2 \cdot 4H_2O$	2 mM	2 mM	2 mM	2 mM
K_2SO_4	0.7 mM	0.7 mM	0.7 mM	0.7 mM
$MgSO_4 \cdot 7H_2O$	0.5 mM	0.5 mM	0.5 mM	0.5 mM
KCl	–	100 μM	–	–
H_3BO_3	10 μM	10 μM	10 μM	10 μM
$ZnSO_4 \cdot 7H_2O$	0.5 μM	0.5 μM	0.5 μM	0.5 μM
$MnSO_4 \cdot H_2O$	0.5 μM	0.5 μM	–	0.5 μM
$CuSO_4 \cdot 5H_2O$	0.2 μM	0.2 μM	0.2 μM	0.2 μM
$(NH_4)_6Mo_7O_{24}$	0.01 μM	0.01 μM	0.01 μM	0.01 μM
Fe-EDTA	20 μM	20 μM	20 μM	–
KH_2PO_4	100 μM	–	100 μM	100 μM

Note: pH was adjusted to 5.7 with KOH.

2 | MATERIALS AND METHODS

2.1 | Hydroponic culture of white lupin

Seeds of *L. albus* L. cv. Amiga were surface-sterilized in 10% H_2O_2 for 30 min, rinsed thoroughly, and soaked in Milli-Q water for 24 h in darkness at 25°C. The soaked seeds were germinated between sheets of filter paper moistened with Milli-Q water for 4 days in darkness at 25°C. Afterward, the seeds were rolled in sheets of filter paper which were transferred vertically to an aerated bucket with distilled water to ensure vertical root growth. From this point, plants were grown in a growth chamber with 16 h light per day (4x Osram Powerstar HQI-T 2000 W/D, 200 μmol m^{-2} s^{-1}), 25/18°C day/night temperature and 55% relative humidity. After 4 days the seedlings were selected for uniform, undamaged and straight growth and transferred to aerated hydroponic systems with 330 ml nutrient solution (Table 1). At day 12, the cotyledons were gently removed to reduce the nutrient supply from seed reserves. The nutrient solution was changed twice a week. At day 20, the Mn treatments began and plants were harvested at day 23. The Mn shock treatment consisted of adding 100 μM $MnSO_4$ to the medium, which is considered a high Mn load (Blamey et al., 2015). The sublethal concentration and relatively short duration of the high-Mn treatment prevented the secondary effects of toxicity. A total of eight treatments was performed (control, P, Mn and Fe; all with and without high-Mn shock), all repeated in seven biological replicates.

2.2 | Elemental analysis by ICP-OES

After harvest, the plant samples were dried at 60°C for 3 days. Roots and one leaf of each of the latest fully expanded leaf pair and the oldest leaf pair (primary leaves) were sampled for each plant. Samples were weighed, digested in 65% HNO_3 (VDLUFA, 2011) and analyzed by optic emission spectroscopy with inductively coupled plasma (ICP-OES; Agilent 5110 SVDV ICP-OES, Agilent Technologies).

2.3 | Phylogenetic analysis

Amino acid sequences of AtMTP proteins, as listed by Ricachenevsky et al. (2013), were acquired by searching the UniProt database (https://www.uniprot.org/). Next, sequences of *A. thaliana* were compared with sequences of *L. albus* using the Basic Local Alignment Search Tool (BLASTp) provided at https://www.whitelupin.fr. Overall, the following 14 genes of *L. albus* were selected according to their alignment scores: Lalb_Chr01g0003451, Lalb_Chr17g0343061, Lalb_Chr12g0210671, Lalb_Chr04g0258611, Lalb_Chr18g0047901, Lalb_Chr06g0163361, Lalb_Chr18g0054081, Lalb_Chr04g0264641, Lalb_Chr15g0085671, Lalb_Chr04g0257941, Lalb_Chr25g0284471, Lalb_Chr01g0015531, Lalb_Chr20g0108461, and Lalb_Chr03g0030331. Sequence alignment and generation of a phylogenetic tree were conducted using the ClustalW algorithm and Neighbor-Joining method in MEGA7, respectively. Tree branches are drawn to scale proportional to evolutionary distances calculated with the Poisson correction model (homogeneous substitution pattern among lineages).

2.4 | Analysis of gene expression in *L. albus* by qRT-PCR

Hundred milligrams of roots, young and old leaves were sampled from three replicates of all treatments, directly frozen in liquid nitrogen, and stored at −80°C. The frozen samples were ground in PL Lysis solution, and RNA was extracted with the innuPREP Plant RNA Kit (Analytik Jena GmbH). RNA was transcribed into cDNA with the QuantiTect Reverse Transcription Kit (Qiagen). Quantitative reverse transcription polymerase chain reaction (qRT-PCR) was performed with a CFX384 Touch Real-Time PCR Detection System (Bio-Rad) and the primers listed in Table 2. For each sample, three technical replicates were performed. The quantification curves were analyzed with CFX Manager 3.0 (Bio-Rad). Protein phosphatase 2A (PP2A) and ubiquitin-conjugating enzyme E2 (UBC) were used as reference genes.

2.5 | Yeast complementation

LaMTP8.1 coding sequence was PCR-amplified from *L. albus* root cDNA by using gene-specific primers and inserted into a USER-compatible pFL61 vector (Minet et al., 1992) by a USER cloning reaction (Nour-Eldin et al., 2006). The pFL61-LaMTP8.1 construct and the empty vector were transformed into a wild-type strain (BY4741) and yeast mutants sensitive to Mn (*pmr1*Δ) or Fe (*ccc1*Δ). Yeast strains were obtained from the Euroscarf collection (Winzeler et al., 1999).

The total RNA was extracted from yeast liquid culture (100 ml SCD-U liquid medium) carrying either empty pFL61 or pFL6-LaMTP8. Yeast cells were broken with glass beads (425–600 μm, acid washed) and lysis buffer (Spectrum Plant Total RNA Kit, Sigma-Aldrich) by using a cell lyser (2010 Geno/Grinder, SPEX). RNA extraction was

TABLE 2 Primers for qPCR and yeast complementation (yc-)

Annotation	Gene[a]	Forward	Reverse
PP2A	Lalb_Chr06g0166161	TGCATGCATAGAGCACCAAG	CATTGTTGAGCTTGCTGAGG
UBC	Lalb_Chr23g0269531	TCGGCGGATCCTGATATTAC	CTGGAACAGAAAAGGCAAGC
LaMTP8.1	Lalb_Chr18g0054081	GTAGAAGCTCGGGAAACAAG	CAAGTGAACCTCCAATACCC
LaMTP8.2	Lalb_Chr15g0085671	CGTTTCTTCCTTACCCATCAG	CAACAGGATCAATCCACCAG
LaIRT1	Lalb_Chr20g0114851	GCTCACCAAGGTAAGTGAAG	CCACATACAACCAGTTATGGG
yc-LaMTP8		GGCTTAAUATGGCTGCAAATTCAGATTC	GGTTTAAUTCAAGGCTGAGAGTTGGGCAG
yc-ScACT3		AAGGATACTGTAGCACTGTTCCCATA	TCCTCCAATATCCATCCTCATCA

[a]Gene sequences for *LaMTP8.1* and *LaIRT1* were obtained from a BLAST of *Arabidopsis* homologs against the White lupin genome (Hufnagel et al., 2020).

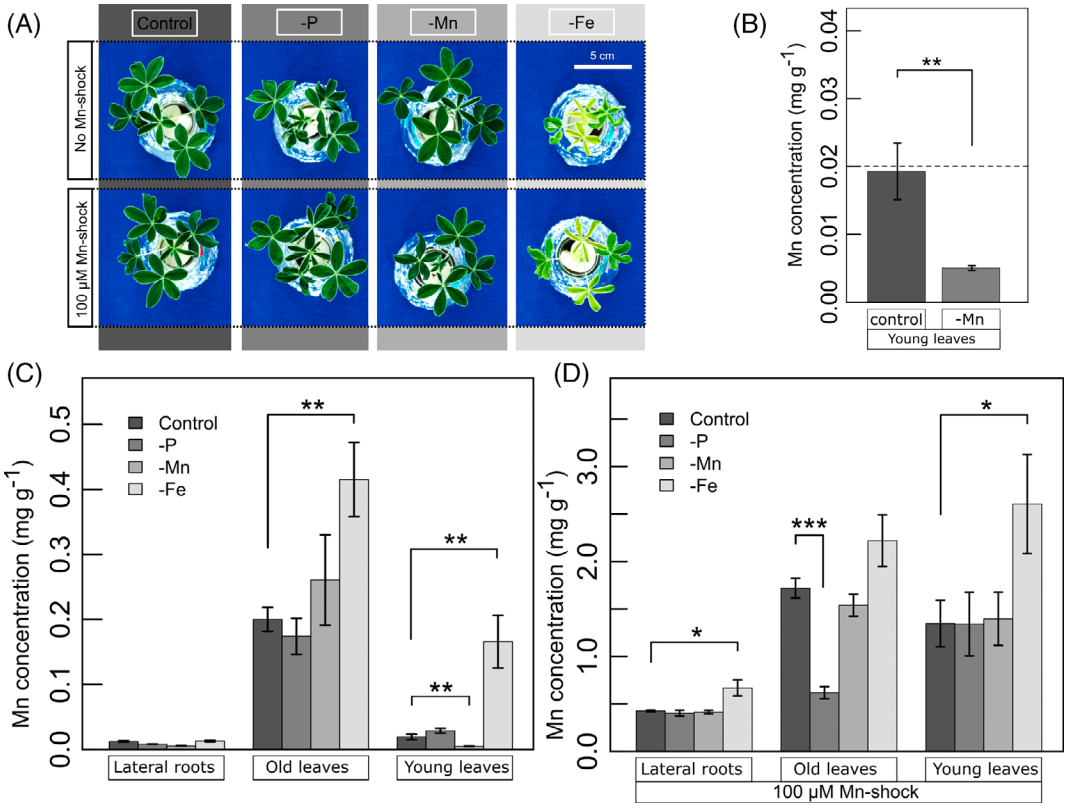

FIGURE 1 (A) Representative images of Lupin plants subjected to different treatments, images were taken just before harvest. Plants were grown in full nutrient solution (control) or in the absence of P, Mn, or Fe. Plants in the upper row were grown without additional Mn and plants in the lower row were treated with 100 μM Mn in the last 3 days. (B) Mn concentrations (mg g^{-1}) in young leaves of nutrient solution-grown white lupins, either in the presence or absence of Mn in the nutrient solution. The dashed line represents the average Mn concentration in Mn-sufficient plants. (C) Mn concentrations (mg g^{-1}) in different tissues of plants grown in full nutrient solution (control) or in the absence of P, Mn, or Fe. (D) Mn accumulation (mg g^{-1}) in different tissues in control plants or P-, Mn-, or Fe-deficient plants after a 3-day treatment with 100 μM Mn. Note the different scales of the *y*-axis. Asterisks indicate significant differences (*p < 0.05, **p < 0.01, ***p < 0.001) between the treatments ($n_{\text{lateral roots}} = 3$, $n_{\text{old leaves}}$, and $n_{\text{young leaves}} = 7$)

performed using the above-mentioned kit following the manufacturer's protocol. The first-strand cDNA was synthesized using M-MuLV Reverse Transcriptase (New England Biolabs) according to the manufacturer's protocol. The PCR reaction conditions were 95°C for 120 s, followed by 30 cycles of 95°C for 10 s, 58°C for 20 s, and 72°C for 90 s. For growth tests, yeast cells were grown in liquid culture overnight at 30°C in SD-Ura medium (2% glucose, 0.2% YNB, 0.5% $[NH_4]_2SO_4$ and 0.08% complete supplement mixture-Ura). Cultures were adjusted to the same OD_{600}, and aliquots were spotted on 2% (w/v) agar plates containing SD-Ura medium as described previously (Peiter, Fischer, et al., 2005a; Peiter, Maathuis, et al., 2005b).

2.6 | Subcellular localization

LaMTP8.1 and *AtMTP8* were cloned into a USER-compatible pART7-mCherry vector (Gleave, 1992) and pART7-mGFP5 vector (Peiter, Fischer, et al., 2005a; Peiter, Maathuis, et al., 2005b), respectively, in frame with a C-terminal mCherry or GFP5 tags to yield 35 S::LaMTP8-mCherry and 35 S::AtMTP8-mGFP5 constructs using appropriate restriction enzymes. The LaMTP8.1-mCherry and AtMTP8-mGFP5 constructs were transiently co-expressed in lupin leaf mesophyll protoplasts as previously described for *A. thaliana* (Eroglu et al., 2016). After transformation, GFP and mCherry fluorescence in protoplasts were observed by confocal laser microscopy using a LSM 880META with a planapochromatic lens (63x/1.4 Oil) (Carl Zeiss). Excitation light source was a 488 nm argon laser (GFP) and a 561 nm diode laser (mCherry). GFP and mCherry fluorescence were detected at emission wavelengths of 499–553 and 588–633 nm, respectively.

2.7 | Statistical analysis

Statistical analysis was conducted in R version 4.0.5 (R Core Team, 2021) with the packages "multcomp" (Version 1.4-12; Hothorn et al., 2008), "s20x" (Version 3.1-31, Balemi et al., 2021), "multcompview" (Version 0.1-8, Graves et al., 2019), and "rcompanion" (Version 2.4.1, Mangiafico, 2021). Data for Figure 1 were analyzed with a Kruskal–Wallis test and post hoc pairwise Wilcoxon rank sum test with Bonferroni correction. Calculation was performed individually for the respective plant tissues. Data from Figures 5 and 6 were analyzed with an ANOVA of a linear mixed effect model with treatment as fixed

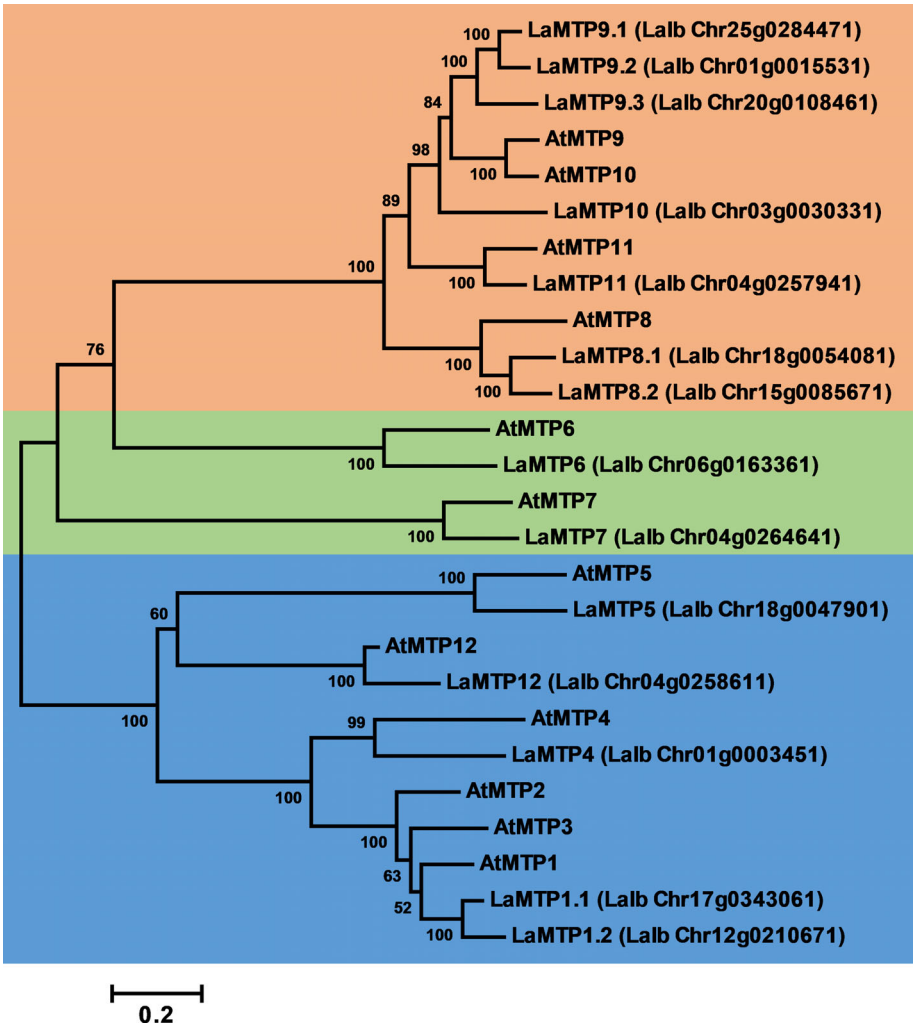

FIGURE 2 Unrooted phylogenetic tree based on the alignment of 26 amino acid sequences of MTP proteins in *A. thaliana* and orthologs in *L. albus*. Colors indicate the assignment of proteins as follows: Zn-CDF (blue), Fe/Zn-CDF (green) and Mn-CDF (orange). Bootstrap values, given as percentages of 1000 bootstrap replications, are noted next to branching points. Horizontal branch lengths are proportional to evolutionary distances calculated with the p-distance method. The scale bar below the tree indicates an evolutionary distance of 0.1 amino acid substitution per position. LaMTP proteins are named according to their Arabidopsis orthologs, except for genes where no clear orthologs can be assigned.

effect and replicate as random effect and Tukey's post hoc test ($p < 0.05$). Analyses were performed individually for the respective plant tissues, and the conditions for the tests performed were checked with Levene's test for homogeneity of variances ($p > 0.05$) and Shapiro–Wilk test for normal distribution of residues ($p > 0.05$).

Statistically significant differences ($p < 0.05$) are indicated with different letters in the figures.

3 | RESULTS

3.1 | Manganese concentrations in Mn-deficient and Mn-shocked lupin tissues

We initially grew white lupins in hydroponic culture for 23 days with full nutrition or without Mn, P, or Fe in the nutrient solution. Fe-deprived plants showed a severely chlorotic phenotype, while seed P reserves were apparently sufficient to support growth for the first 3 weeks (Figure 1A). When Mn was omitted from the growth solution, the seed pool of Mn was sufficient to support normal growth for more than 3 weeks, but the Mn concentrations in young leaves were already very low, indicating Mn deficiency in this tissue (Figure 1B). We measured Mn concentrations in roots, young leaves, and old leaves. The latter had about 10-fold higher Mn concentrations than roots or young leaves, indicative of Mn accumulation in the old leaves. The Fe-deficient plants had higher Mn concentrations in the shoot, both in young and old leaves, while P deficiency did not affect Mn accumulation (Figure 1C).

Plants of all treatments were then exposed to a 100 μM Mn shock for 3 days. As expected, Mn concentrations in roots and especially in shoots were substantially increased by this Mn exposure (Figure 1C,D; note the different scales in sub-figures). In roots and in young leaves, Mn accumulated to higher levels in Fe plants than in control plants, while this was not observed in P- or Mn-starved plants exposed to high Mn. In old leaves, by contrast, there was a lower accumulation of Mn in P-deprived plants than in controls. After the Mn shock, similar Mn concentrations were measured in young and old leaves of the P-deprived plants.

3.2 | Identification of the CDF protein family of metal transporters in white lupin

The strong accumulation of Mn in old leaves of white lupin opened the possibility that an ortholog of MTP8 might be involved in Mn accumulation and sequestration. We therefore scanned the genome of white lupin for CDF members. BLAST searches against all Arabidopsis CDFs identified 14 genes of this family. Based on their similarity with characterized members in *A. thaliana*, they grouped into three clades (Figure 2). A phylogenetic tree drawn to scale with horizontal branch lengths as evolutionary distances indicates an assignment to the following groups of the classification by Ricachenevsky et al. (2013): Zn-CDF (blue, five members), Fe/Zn-CDF (green, two members), and Mn-CDF (orange, seven members). Overall, five, two and seven proteins of *L. albus* were classified as members of the Zn-CDF, Fe/Zn-CDF, and Mn-CDF group, respectively, whereas for *A. thaliana*, six, two, and four proteins belong to these groups. Two close homologs were found for AtMTP1, AtMTP2, and AtMTP3, whereas one homolog was found for AtMTP4. Moreover, AtMTP5, AtMTP6, AtMTP7, AtMTP11, and AtMTP12 have one close homolog each. Concerning AtMTP8 and AtMTP11, two and one close homologs were identified, respectively. Regarding the group containing AtMTP9 and AtMTP10, three lupin homologs were identified and named LaMTP9.1, LaMTP9.2, and LaMTP9.3.

3.3 | LaMTP8.1 functions as Mn and Fe transporter in yeast

The MTP8 orthologs present in the white lupin genome were candidates for the Mn accumulation mechanism in old leaves. In a preliminary gene expression analysis of whole plants, we detected the expression of Lalb_Chr18g0054081, amplified its open reading frame from a *L. albus* cDNA library, and called this gene *LaMTP8.1*, based on its homology to AtMTP8. The ORF was cloned into a yeast expression vector and expressed in the *pmr1*Δ yeast mutant

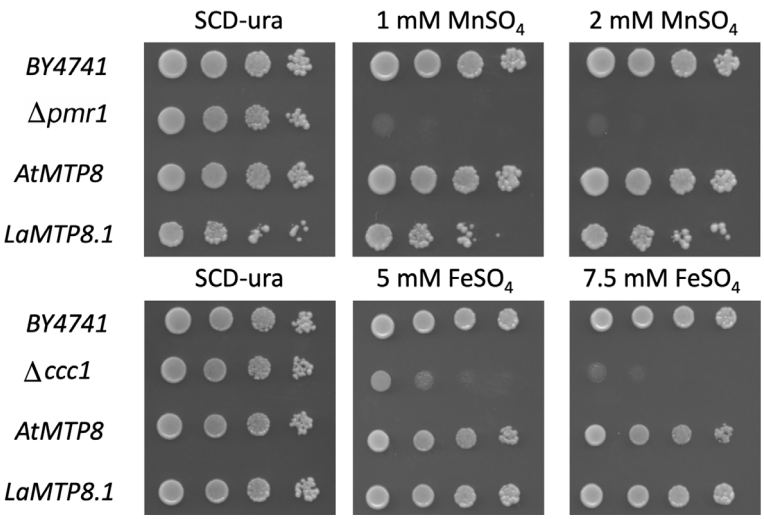

FIGURE 3 Growth rescue of wild-type and mutant yeast strains sensitive to Mn (*pmr1*Δ, upper panels) and Fe (*ccc1*Δ, lower panels) by expression of *LaMTP8.1* and *AtMTP8* as positive control. A series of 10-fold dilutions was dropped onto SCD-Ura plates. Concentrations of metals in the growth medium are indicated in the figure.

(Figure S1). *LaMTP8.1* rescued the growth of this strain on elevated, toxic Mn concentrations, suggesting a function in Mn transport and detoxification (Figure 3). Furthermore, the growth of the yeast *ccc1*Δ mutant, sensitive to high external Fe, was rescued by LaMTP8.1, implicating a potential function also in Fe detoxification, similar to AtMTP8.

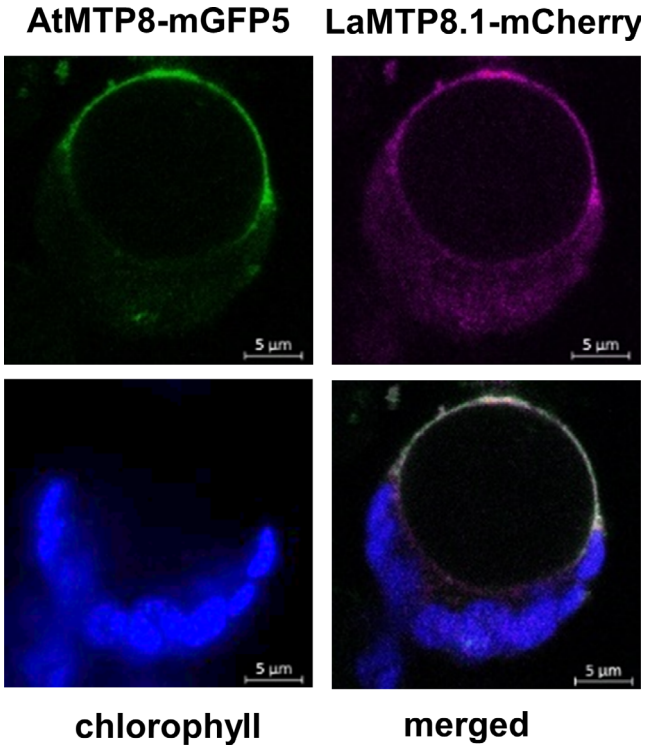

FIGURE 4 LaMTP8.1-mCherry co-localizes with AtMTP8-mGFP5 to the vacuolar membrane in mesophyll cells of white lupin. Mesophyll protoplasts of white lupin were co-transformed with LaMTP8.1-mCherry and AtMTP8-mGFP5 and fluorescence was observed by confocal laser scanning microscopy. The images are representative of 100 cells examined in three independently performed imaging experiments. Non-vacuolar localization of LaMTP8.1-mCherry has not been observed. Scale bar: 5 µm.

3.4 | LaMTP8.1 localizes to the tonoplast

Most MTP8 orthologues in other species operate in the tonoplast, which made them good candidate for vacuolar sequestration of Mn. The metal detoxification phenotypes in the heterologous host yeast supported such a function for LaMTP8.1 in white lupin. Therefore, we hypothesized that LaMTP8.1 localized in the tonoplast and tested this in white lupin mesophyll protoplasts as a homologous expression system to avoid the mislocalization artifacts of heterologous systems. Indeed, the mCherry-tagged LaMTP8.1 co-localized with the vacuolar marker AtMTP8-mGFP5 in the vacuolar membrane, confirming our hypothesis (Figure 4). Taken together, the function of LaMTP8.1 in yeast and its localization in the vacuolar membrane indicate a role in vacuolar sequestration of Mn, and possibly also Fe.

3.5 | Tissue-specific *LaMTP8.1* expression is upregulated by excessive Mn

The physiological role of *LaMTP8.1* depends on its transcriptional regulation. Quantitative RT-PCR analyses showed that *LaMTP8.1* was expressed in roots and shoots (Figure 5). In young and old leaves, but not in roots, expression was elevated under Fe deficiency (Figure 5A). Furthermore, *LaMTP8.1* expression was substantially increased in all tissues, but particularly in old leaves, after high-Mn treatment (Figure 5B). This transcriptional activation in leaves under Fe deficiency and high Mn load coincides with the elevated Mn accumulation under those conditions (Figure 1), further supporting a role of LaMTP8.1 in Mn sequestration.

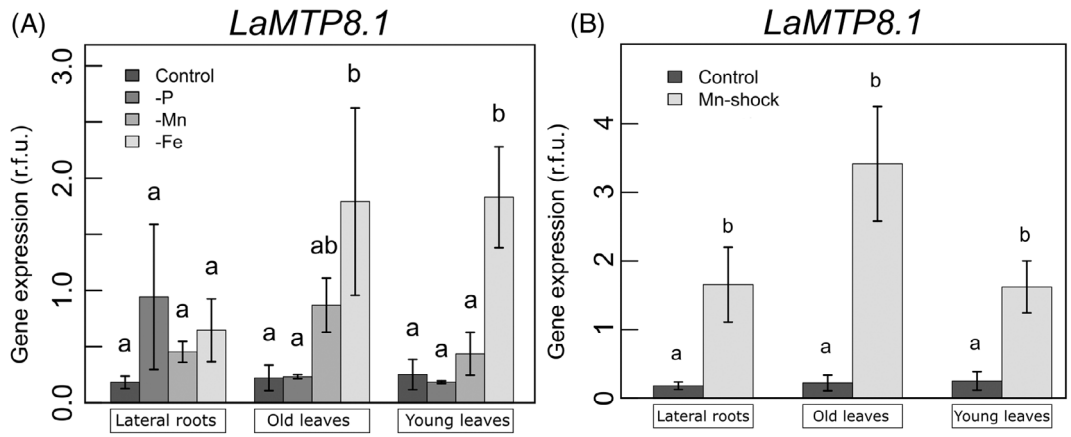

FIGURE 5 Expression of *LaMTP8.1* in roots, old leaves and young leaves of plants grown (a) in full nutrient solution (control) or in the absence of P, Mn, or Fe or (B) after a 3-day treatment of control plants with 100 µM Mn. Expression was determined by qRT-PCR and normalized to *PP2A* and *UBC* as reference genes. Different letters indicate significant differences ($p < 0.05$) between the treatments within one tissue ($n_{biological} = 3$, $n_{technical} = 3$).

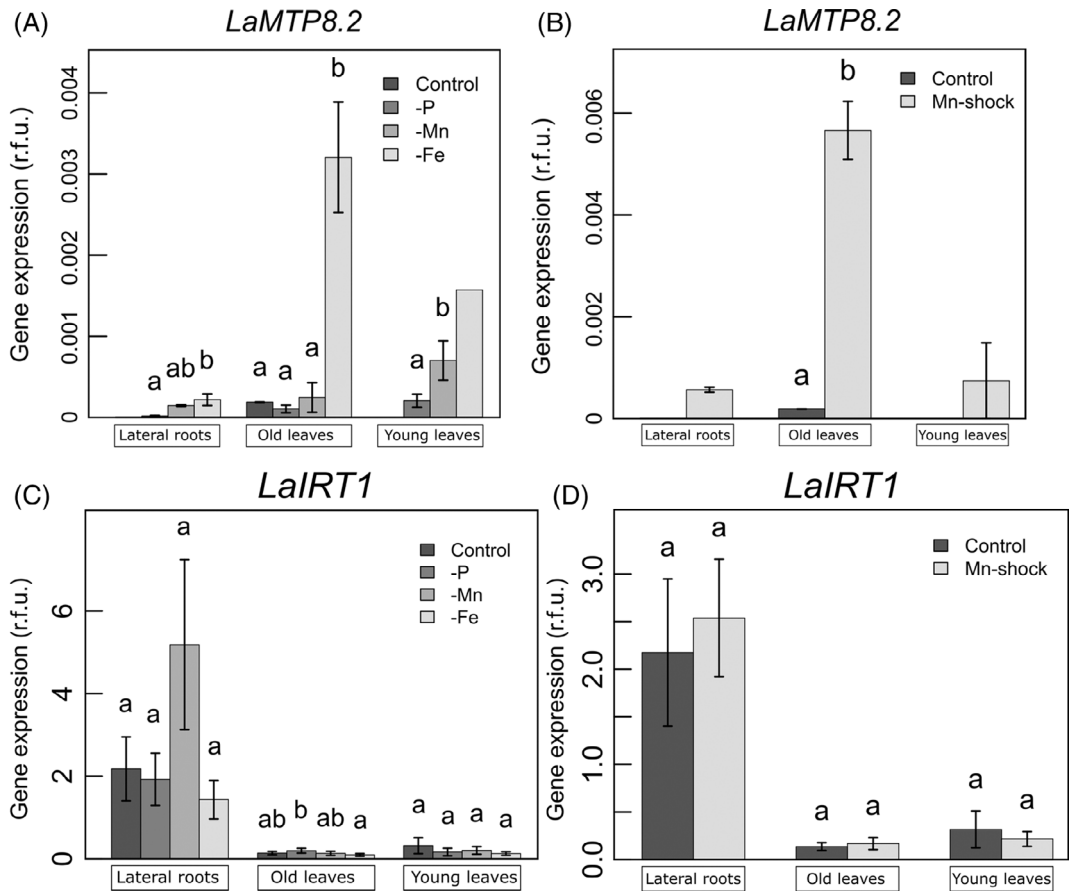

FIGURE 6 Expression of *LaMTP8.2* (A, B) and *LaIRT1* (C, D) in roots, old leaves and young leaves of plants grown (A, C) in full nutrient solution (control) or in the absence of P, Mn, or Fe or (B, D) after a 3-day treatment of control plants with 100 μM Mn. Expression was determined by qRT-PCR and normalized to *PP2A* and *UBC* as housekeeping genes. Different letters indicate significant differences ($p < 0.05$) between the treatments within one tissue ($n_{biological} = 3$, $n_{technical} = 3$), statistics are incomplete due to insufficient values for the low-expressed *LaMTP8.2*.

3.6 | Expression of related genes and relationship with iron

The white lupin genome encodes another MTP8 orthologue, LaMTP8.2, which might also be involved in Mn accumulation by old leaves. Similar to *LaMTP8.1*, the expression of *LaMTP8.2* was increased by Fe deficiency and by Mn excess (Figure 6). However, transcript levels were about 100x lower than those of *LaMTP8*, and undetectable in some replicates. Therefore, LaMTP8.2 likely plays a minor role under the conditions studied, but may have a conditional role under yet unknown conditions.

We additionally measured Fe concentrations in roots and shoots of P-, Mn-, and Fe-deficient and high Mn-treated plants. In contrast to Mn (Figure 1), Fe concentration was higher in the root dry matter than in the aerial plant parts, probably due to Fe precipitation in the root apoplast, which is commonly observed (Figure S2). Interestingly, Fe deficiency caused an increase in Mn (Figure 1), while Mn deficiency, by contrast, did not cause an increase in Fe (Figure S2).

Uptake of Fe and Mn may be mediated by the IRT1 orthologue of white lupin, LaIRT1. We, therefore, analyzed the expression of *LaIRT1*, which was almost exclusively expressed in roots. *LaIRT1* transcript level tended to be higher under Mn deficiency (although not significantly) but not after prolonged Fe deficiency (Figure 6C) leading to severe chlorosis (Figure 1A). As may have been expected from unchanged Fe concentrations in lupin tissues after the Mn shock, the high-Mn treatment did not have an influence on *LaIRT1* expression (Figure 6D).

4 | DISCUSSION

White lupin builds up very high amounts of Mn in its leaves without suffering from toxicity, as most plants would do at such concentrations (Peiter et al., 2000). In soil, this Mn accumulation is strongly promoted under P deficiency, which induces a massive release of acidifying and reducing compounds by cluster roots. The mechanistic basis of Mn detoxification in white lupin leaves has been unknown. Owing to its function in Mn detoxification in other species (Eroglu et al., 2016; Li et al., 2021; Takemoto et al., 2017), we hypothesized that an ortholog of the vacuolar Mn transporter MTP8 may adopt this physiological role. In *Arabidopsis*, MTP8 determines Mn homeostasis in specific contexts and tissues, in particular in Fe-deficient roots and in developing embryos, but it is largely absent from leaves (Eroglu et al., 2016, 2017).

We identified *LaMTP8.1* as the most highly expressed one of two orthologs of *AtMTP8* in white lupin (Figure 5). The expression of a second orthologue, *LaMTP8.2*, was very low, albeit regulated similarly to *LaMTP8.1* (Figure 6). Functional analysis of LaMTP8.1 in yeast mutants sensitive to elevated Mn and Fe concentrations indicated a potential function in the transport of those elements (Figure 3). It should be noted that *in planta*, transport activity would depend on the presence of the cations in their free divalent form in the cytosol, which is likely to be minuscule for Fe because of its strong chelation with other compounds (Connorton et al., 2017). Its localization to the tonoplast suggests that LaMTP8.1 mediates the sequestration of Mn into vacuoles like its Arabidopsis counterpart (Figure 4). Similar to Arabidopsis MTP8 (Eroglu et al., 2016), LaMTP8.1 is likely not relevant for Fe accumulation in leaf vacuoles.

LaMTP8.1 expression was little affected by Mn-deficient conditions (Figure 5), whereas it was strongly elevated under Fe deficiency and even more so after exposure to high Mn levels (Figure 5). Unlike in Arabidopsis, this transcriptional activation was not confined to roots but extended to leaves. In parallel to the increased *LaMTP8* expression, Mn concentrations were substantially affected by variations in the Mn supply (Figure 1). However, *LaMTP8.1* expression strength did not reflect the preferential accumulation of Mn in old leaves of plants grown under control conditions. This suggests the operation of further mechanisms of Mn allocation that may act on, upstream of, or in parallel to *LaMTP8*, similar to what has been observed in Mn distribution in Arabidopsis embryos (Höller et al., 2022).

Interestingly, Fe deficiency significantly increased the leaf Mn concentration (Figure 1). This interaction has been described before in Arabidopsis, where it is explained by the poor selectivity of the Fe uptake transporter IRT1, which is strongly upregulated by limited Fe supply (Korshunova et al., 1999). Although strong Fe deficiency was observed in the Fe-deprived lupins—detectable both by severe leaf chlorosis and drastically reduced Fe concentrations in the plant tissues—the expression of *LaIRT1* did not increase in the present study (Figure 6). This observation may be explained by the transient nature of *IRT1* upregulation in response to Fe deficiency. In Arabidopsis, *IRT1* expression declines again after a few days because a minimum amount of Fe is required to execute the Fe deficiency response at the transcriptional level (Connolly et al., 2002; Vert et al., 2003). Since lupin plants grew in Fe-deficient conditions for the entire culture period, the primary Fe reserves of the seed were quickly depleted, and an initially increased *LaIRT1* expression may have been missed at the time of harvest.

In Arabidopsis, *AtMTP8* expression is induced in the *IRT1*-expressing root cells, sequestering Mn at the point of its unwanted uptake (Eroglu et al., 2016). Intriguingly, *AtMTP8* is even an integral part of the Fe deficiency response, being regulated by the Fe deficiency-induced transcription factor FIT. Upregulation of *AtMTP8* by high Mn levels in the growth medium is also FIT-dependent, which may be explained by the plant's perception of Mn toxicity as an induced Fe deficiency. Our experiments indicate that the Mn–Fe antagonism in white lupin differs markedly from that in Arabidopsis. Importantly, the expression of *LaMTP8.1* under low Fe and high Mn was not confined to the roots but also very prominent in the leaves. This indicates only a minor, if any, role of a FIT orthologue in the regulation of *LaMTP8.1*. Furthermore, high Mn availability also provoked an upregulation of *LaMTP8.1* without activating *LaIRT1*, and, notably, without decreasing Fe levels. These data suggest that under high Mn availability, *LaMTP8.1* is upregulated directly by Mn and not by a response to Mn-induced Fe deficiency. The mechanistic basis of such a Mn-dependent transcriptional regulation is unknown at present.

It had been hypothesized that the Mn concentration in the leaves can be used as a proxy for P efficiency of various species because of carboxylate exudation due to P deficiency and concomitant Mn solubilization and uptake (Lambers et al., 2015, 2021; Pang et al., 2018). In the hydroponic experiments of this study, Mn concentrations were not increased in P-deficient plants as compared to controls (Figure 1). This underlines that increased Mn concentrations in soil-grown P-deficient white lupins are indeed due to Mn mobilization from the soil matrix rather than due to a merely increased Mn uptake capacity. Importantly, the expression of *LaMTP8.1* was also not changed under P-deficient conditions (Figure 5). Albeit Mn detoxification being an integral part of the P deficiency response in *L. albus*, the transcriptional activation of this transporter is not under direct control of the P deficiency network, but again regulated indirectly by high Mn availability.

LaMTP8.1 most likely functions as a Mn transporter that mediates vacuolar Mn sequestration in *L. albus*. The expression of *LaMTP8.1* coincided with high Mn concentrations in leaves of plants challenged with Fe deficiency and Mn surplus, thus LaMTP8.1 activity is the most likely mechanism for Mn accumulation in P-deficient soil-grown white lupins. The regulation of *LaMTP8.1* reveals a notable difference in Mn handling of white lupin compared *to Arabidopsis*. Arabidopsis copes with Mn influx only at the point of entry into Fe-deficient plants, white lupin utilizes LaMTP8.1 to safely store Mn also in leaf tissues, a strategy that resembles the one employed by rice, where it also involves MTP8 orthologs.

AUTHOR CONTRIBUTIONS

Philipp Olt, Edgar Peiter, and Uwe Ludewig designed the experiments, Philipp Olt, Santiago Alejandro, Johann Fermum, and Edith Ramos conducted the experiments and analyzed the data, Philipp Olt, Edgar Peiter, and Uwe Ludewig wrote the paper.

ACKNOWLEDGMENTS

We thank Tina Peiter-Volk for excellent technical support and Ashvin Mohan for assistance in the experiments. This work was supported by the European Regional Development Fund (ERDF) within the State Research Focus Program "Molecular Biosciences as a Motor for a Knowledge-Based Economy" (ZS/2016/06/79740 to E.P.) and by the German Research Foundation (DFG, grants Lu673/25-1 to Uwe Ludewig and INST271/371-1 FUGG to Ingo Heilmann). Open Access funding enabled and organized by Projekt DEAL.

DATA AVAILABILITY STATEMENT

The data that support the findings of this study are available from the corresponding author upon reasonable request.

ORCID

Philipp Olt https://orcid.org/0000-0003-2738-8722

Santiago Alejandro-Martinez https://orcid.org/0000-0001-5487-8183

Edgar Peiter https://orcid.org/0000-0002-9104-3238

Uwe Ludewig https://orcid.org/0000-0001-5456-1055

REFERENCES

Alejandro, S., Höller, S., Meier, B. & Peiter, E. (2020) Manganese in plants: from acquisition to subcellular allocation. *Frontiers in Plant Science*, 11, 300.

Andresen, E., Peiter, E. & Küpper, H. (2018) Trace metal metabolism in plants. *Journal of Experimental Botany*, 69, 909–954.

Balemi, A., Chandra, D., Curran, J., Deppa, B., Forster, M., Maia, C., et al. (2021). Package 's20x': functions for University of Auckland Course STATS 201/208 data analysis. R package version 3.1-31.

Barber, J. (2017) A mechanism for water splitting and oxygen production in photosynthesis. *Nature Plants*, 3(4), 1–5.

Blamey, F.P.C., Hernandez-Soriano, M.C., Cheng, M., Tang, C., Paterson, D. J., Lombi, E. et al. (2015) Synchrotron-based techniques shed light on mechanisms of plant sensitivity and tolerance to high manganese in the root environment. *Plant Physiology*, 169(3), 2006–2020.

Blamey, F.P.C., McKenna, B.A., Li, C., Cheng, M., Tang, C., Jiang, H. et al. (2018) Manganese distribution and speciation help to explain the effects of silicate and phosphate on manganese toxicity in four crop species. *New Phytologist*, 217(3), 1146–1160.

Buczko, U., van Laak, M., Eichler-Löbermann, B., Gans, W., Merbach, I., Panten, K. et al. (2018) Re-evaluation of the yield responses to phosphorus fertilization based on meta-analyses of long-term field experiments. *Ambio*, 47, S50–S61.

Cailliatte, R., Schikora, A., Briat, J.F., Mari, S. & Curie, C. (2010) High-affinity manganese uptake by the metal transporter NRAMP1 is essential for Arabidopsis growth in low manganese conditions. *The Plant Cell*, 22(3), 904–917.

Castaings, L., Caquot, A., Loubet, S. & Curie, C. (2016) The high-affinity metal transporters NRAMP1 and IRT1 team up to take up iron under sufficient metal provision. *Scientific Reports*, 6(1), 1–11.

Chen, Z., Fujii, Y., Yamaji, N., Masuda, S., Takemoto, Y., Kamiya, T. et al. (2013) Mn tolerance in rice is mediated by MTP8. 1, a member of the cation diffusion facilitator family. *Journal of Experimental Botany*, 64(14), 4375–4387.

Connolly, E.L., Fett, J.P. & Guerinot, M.L. (2002) Expression of the IRT1 metal transporter is controlled by metals at the levels of transcript and protein accumulation. *The Plant Cell*, 14(6), 1347–1357.

Connorton, J.M., Balk, J. & Rodríguez-Celma, J. (2017) Iron homeostasis in plants—a brief overview. *Metallomics*, 9(7), 813–823.

Delhaize, E., Kataoka, T., Hebb, D.M., White, R.G. & Ryan, P.R. (2003) Genes encoding proteins of the cation diffusion facilitator family that confer manganese tolerance. *The Plant Cell*, 15(5), 1131–1142.

Dinkelaker, B., Hengeler, C., Neumann, G., Eltrop, L. & Marschner, H. (1997) Root exudates and mobilization of nutrients. *Trees-Contributions to Modern Tree Physiology*, 441–452.

Eroglu, S., Meier, B., von Wirén, N. & Peiter, E. (2016) The vacuolar manganese transporter MTP8 determines tolerance to iron deficiency-induced chlorosis in Arabidopsis. *Plant Physiology*, 170(2), 1030–1045.

Eroglu, S., Giehl, R., Meier, B., Takahashi, M., Terada, Y., Ignatyev, K. et al. (2017) Metal tolerance protein 8 mediates manganese homeostasis and iron re-allocation during seed development and germination. *Plant Physiology*, 174, 1633–1647.

Gleave, A.P. (1992) A versatile binary vector system with a T-DNA organisational structure conducive to efficient integration of cloned DNA into the plant genome. *Plant Molecular Biology*, 20(6), 1203–1207.

Graves, S., Piepho, H.P., Selzer, L. & Dorai-Raj, S. (2019) *multcompView: visualizations of paired comparisons. R package c*. Vienna, Austria: R Foundation for Statistical Computing.

He, J., Rössner, N., Hoang, M.T.T., Alejandro, S. & Peiter, E. (2021) Transport, functions, and interactions of calcium and manganese in plant organellar compartments. *Plant Physiology*, 187, 1940–1972.

Höller, S., Küpper, H., Brückner, D., Garrevoet, J., Spiers, K., Falkenberg, G. et al. (2022) Overexpression of *METAL TOLERANCE PROTEIN8* reveals new aspects of metal transport in *Arabidopsis thaliana* seeds. *Plant Biology*, 24, 23–29.

Horiguchi, T. (1988) Mechanism of manganese toxicity and tolerance of plants: IV. Effects of silicon on alleviation of manganese toxicity of rice plants. *Soil Science and Plant Nutrition*, 34(1), 65–73.

Hothorn, T., Bretz, F. & Westfall, P. (2008) Simultaneous inference in general parametric models. *Biometrical Journal: Journal of Mathematical Methods in Biosciences*, 50(3), 346–363.

Hufnagel, B., Marques, A., Soriano, A., Marquès, L., Divol, F., Doumas, P. et al. (2020) High-quality genome sequence of white lupin provides insight into soil exploration and seed quality. *Nature Communications*, 11(1), 1–12.

Ju, C., Zhang, Z., Deng, J., Miao, C., Wang, Z., Wallrad, L. et al. (2022) Ca^{2+}-dependent successive phosphorylation of vacuolar transporter MTP8 by CBL2/3-CIPK3/9/26 and CPK5 is critical for manganese homeostasis in Arabidopsis. *Molecular Plant*, 15(3), 419–437.

Kania, A., Langlade, N., Martinoia, E. & Neumann, G. (2003) Phosphorus deficiency-induced modifications in citrate catabolism and in cytosolic pH as related to citrate exudation in cluster roots of white lupin. *Plant and Soil*, 248(1), 117–127.

Korshunova, Y.O., Eide, D., Clark, W.G., Guerinot, M.L. & Pakrasi, H.B. (1999) The IRT1 protein from Arabidopsis thaliana is a metal transporter with a broad substrate range. *Plant Molecular Biology*, 40(1), 37–44.

Lambers, H., Hayes, P.E., Laliberte, E., Oliveira, R.S. & Turner, B.L. (2015) Leaf manganese accumulation and phosphorus-acquisition efficiency. *Trends in Plant Science*, 20(2), 83–90.

Lambers, H., Wright, I.J., Pereira, C.G., Bellingham, P.J., Bentley, L.P., Boonman, A. et al. (2021) Leaf manganese concentrations as a tool to assess belowground plant functioning in phosphorus-impoverished environments. *Plant and Soil*, 461(1), 43–61.

Li, J., Zheng, L., Fan, Y., Wang, Y., Ma, Y., Gu, D. et al. (2021) Pear metal transport protein PbMTP8. 1 confers manganese tolerance when expressed in yeast and *Arabidopsis thaliana*. *Ecotoxicology and Environmental Safety*, 208, 111687.

Loneragan, J.F. (1988) Distribution and movement of manganese in plants. In: *Manganese in soils and plants*. Dordrecht: Springer, pp. 113–124.

Mangiafico, S. (2021) rcompanion: functions to support extension education program evaluation. R package version 2.4.1.

McHargue, J.S. (1922) The role of manganese in plants. *Journal of the American Chemical Society*, 44(7), 1592–1598.

Minet, M., Dufour, M.E. & Lacroute, F. (1992) Complementation of Saccharomyces cerevisiae auxotrophic mutants by Arabidopsis thaliana cDNAs. *The Plant Journal*, 2(3), 417–422.

Montanini, B., Blaudez, D., Jeandroz, S., Sanders, D. & Chalot, M. (2007) Phylogenetic and functional analysis of the cation diffusion facilitator (CDF) family: improved signature and prediction of substrate specificity. *BMC Genomics*, 8(1), 1–16.

Nour-Eldin, H.H., Hansen, B.G., Nørholm, M.H.H., Jensen, J.K. & Halkier, B.A. (2006) Advancing uracil-excision based cloning towards an ideal technique for cloning PCR fragments. *Nucleic Acids Research*, 34, e122.

Ono, T.A., Noguchi, T., Inoue, Y., Kusunoki, M., Matsushita, T. & Oyanagi, H. (1992) X-ray detection of the period-four cycling of the manganese cluster in photosynthetic water oxidizing enzyme. *Science*, 258(5086), 1335–1337.

Pang, J., Bansal, R., Zhao, H., Bohuon, E., Lambers, H., Ryan, M.H. et al. (2018) The carboxylate-releasing phosphorus-mobilizing strategy can be proxied by foliar manganese concentration in a large set of chickpea germplasm under low phosphorus supply. *New Phytologist*, 219(2), 518–529.

Pedas, P., Schiller Stokholm, M., Hegelund, J.N., Ladegård, A.H., Schjoerring, J.K. & Husted, S. (2014) Golgi localized barley MTP8 proteins facilitate Mn transport. *PLoS One*, 9(12), e113759.

Peiter, E. (2014) Mineral deficiencies. In: Krauss, G.-J. & Niess, D.H. (Eds.) *Ecological biochemistry—environmental and interspecies interactions*. Weinheim, Germany: Wiley-VCH, pp. 209–222.

Peiter, E., Yan, F. & Schubert, S. (2000) Are mineral nutrients a critical factor for lime intolerance of lupins? *Journal of Plant Nutrition*, 23, 617–635.

Peiter, E., Fischer, M., Sidaway, K., Roberts, S.K. & Sanders, D. (2005a) The *Saccharomyces cerevisiae* Ca^{2+} channel Cch1pMid1p is essential for tolerance to cold stress and iron toxicity. *FEBS Letters*, 579(25), 5697–5703.

Peiter, E., Maathuis, F.J.M., Mills, L.N., Knight, H., Pelloux, J., Hetherington, A.M. et al. (2005b) The vacuolar Ca^{2+}-activated channel TPC1 regulates germination and stomatal movement. *Nature*, 434, 404–408.

Peiter, E., Montanini, B., Gobert, A., Pedas, P., Husted, S., Maathuis, F.J.M. et al. (2007) A secretory pathway-localized cation diffusion facilitator confers plant manganese tolerance. *Proceedings of the National Academy of Sciences of the United States of America*, 104, 8532–8537.

R Core Team. (2021) *R: a language and environment for statistical computing*. Vienna, Austria: R Foundation for Statistical Computing.

Rengel, Z. (2000) Manganese uptake and transport in plants. *Metal Ions in Biological Systems*, 37, 57–87.

Ricachenevsky, F.K., Menguer, P.K., Sperotto, R.A., Williams, L.E. & Fett, J.P. (2013) Roles of plant metal tolerance proteins (MTP) in metal storage and potential use in biofortification strategies. *Frontiers in Plant Science*, 4, 144.

Rogers, E.E., Eide, D.J. & Guerinot, M.L. (2000) Altered selectivity in an Arabidopsis metal transporter. *Proceedings of the National Academy of Sciences of the United States of America*, 97(22), 12356–12360.

Takemoto, Y., Tsunemitsu, Y., Fujii-Kashino, M., Mitani-Ueno, N., Yamaji, N., Ma, J.F. et al. (2017) The tonoplast-localized transporter MTP8.2 contributes to manganese detoxification in the shoots and roots of *Oryza sativa* L. *Plant and Cell Physiology*, 58(9), 1573–1582.

VDLUFA (2011) Methode 2.1.1 Nassaufschluss unter Druck. Methodenbuch Band VII, 4. Auflage (Umweltanalytik).

Vert, G., Grotz, N., Dédaldéchamp, F., Gaymard, F., Guerinot, M.L., Briat, J.F. et al. (2002) IRT1, an Arabidopsis transporter essential for iron uptake from the soil and for plant growth. *The Plant Cell*, 14(6), 1223–1233.

Vert, G.A., Briat, J.F. & Curie, C. (2003) Dual regulation of the Arabidopsis high-affinity root iron uptake system by local and long-distance signals. *Plant Physiology*, 132(2), 796–804.

Wang, Z., Shen, J., Ludewig, U. & Neumann, G. (2015) A re-assessment of sucrose signaling involved in cluster-root formation and function in phosphate-deficient white lupin (Lupinus albus). *Physiologia Plantarum*, 154(3), 407–419.

White, P.J. & Neugebauer, K. (2021) Possible consequences of an inability of plants to control manganese uptake. *Plant and Soil*, 461(1), 63–68.

White, P.J. & Pongrac, P. (2017) Heavy-metal toxicity in plants: Mercury (Hg). *Plant Stress Physiology*, 2(5), 300.

Winzeler, E.A., Shoemaker, D.D., Astromoff, A., Liang, H., Anderson, K., Andre, B. et al. (1999) Functional characterization of the *S. cerevisiae* genome by gene deletion and parallel analysis. *Science*, 285(5429), 901–906.

Zhang, Z., Fu, D., Sun, Z., Ju, C., Miao, C., Wang, Z. et al. (2021) Tonoplast-associated calcium signaling regulates manganese homeostasis in *Arabidopsis*. *Molecular Plant*, 14(5), 805–819.

SUPPORTING INFORMATION

Additional supporting information can be found online in the Supporting Information section at the end of this article.

How to cite this article: Olt, P., Alejandro-Martinez, S., Fermum, J., Ramos, E., Peiter, E. & Ludewig, U. (2022) The vacuolar transporter LaMTP8.1 detoxifies manganese in leaves of *Lupinus albus*. *Physiologia Plantarum*, 174(6), e13807. Available from: https://doi.org/10.1111/ppl.13807